Research Note

Seismic Evaluation of Steel Frames Subjected to Decaying Sinusoidal Records through IDA Method

Mehdi Hemmat[1], Seyed Shaker Hashemi[2*], and Mohammad Vaghefi[3]

1. M.Sc. Graduated, Structural Engineering, Persian Gulf University, Iran
2. Assistant Professor, Department of Civil Engineering, Persian Gulf University, Iran,
* Corresponding Author; email: Sh.hashemi@pgu.ac.ir
3. Assistant Professor, Department of Civil Engineering, Persian Gulf University, Iran

Received: 26/11/2013
Accepted: 21/05/2014

ABSTRACT

The focus of this paper is on the responses of steel moment resisting frames to pulse-like near-fault ground motions. Decaying sinusoidal record is a simulated record that possesses specifications of real pulse-like near-fault earthquake. Incremental Dynamic Analysis (IDA) is a new approach of dynamic analysis that is appropriate for assessment of the structural performance. IDA is performed on steel moment resisting frames with different heights subjected to real and simulated records. PGV is employed as a suitable intensity measure for pulse-like near-fault records. Results show that at the low intensity of excitations, decaying sinusoidal record is a suitable alternative for pulse-like near-fault records. Besides, the response to the decaying sinusoidal records shows lower scattering than the responses to the real records especially when PGV is used as the intensity measure. Moreover, the structural responses under decaying sinusoidal records show strong dependency of this simulated record to the pulse frequency.

Keywords:
Incremental dynamic analysis; Moment-resisting steel frames; Near-fault motion; Simulated decaying sinusoidal records

1. Introduction

Incremental Dynamic Analysis (IDA) is an emerging analysis method that offers through seismic demand and capacity prediction capability by using a series of nonlinear dynamic analyses under a multiply scaled suite of ground motion records [1]. In other words, IDA is a parametric method that contains one or more records scaled from low to high intensity and persuade structures to cover a wide range from elasticity to global dynamic failure. An appropriate model for the structure under investigation is required to perform an IDA. In addition, a suite of ground motion records is selected, for each record incrementally scale it to multiple levels and run a nonlinear dynamic analysis each time since numerical non-convergence is first encountered. A ground motion intensity measure (IM) such as $S_a(T_1, 5\%)$ or PGA and a Damage Measure (DM) such as the maximum over all stories peak interstory drift ratio (θ_{max}) is selected. By interpolating the resulting IM and DM points for each individual record, an IDA curve will be generated as the final result [2]. By evaluating an IDA curve, a thorough understanding of the range of needs to development of records and a proper understanding of the structural response changes such as increasing ground motion intensity are obtained. In addition, it is feasible to provide an estimate of overall system capacity [1-2].

In a dynamic analysis, the responses of the structure depend on the nature of ground motions.

To better explain, accelerograms which used to determine the effect of ground motion should be possible to represent the actual movement of the site. For example, to perform IDA for structures located on the near-fault region, it is better to use near-fault records. Near-field regions are very important in comparison with far-field district because of the fact that near-fault records have the following unique features:

1. Values of PGA and PGV in near-fault records are higher than far-fault records.
2. Long period pulse is observed at the beginning of records that is evident in the normal component to the fault plane.
3. In the fault normal component, PGV has greater values than the parallel component [3].
4. Because of the accumulation of shear waves in the forward directivity and the long period pulses, the amount of energy released in front of forward directivity is extremely high [4].

It is clear that near-fault ground motions need more attention since they caused severe damage to structures, especially those which are located in the path of forward-directivity [5]. Many parameters affect the near-fault ground motions, such as fault mechanisms, the route of failure, and the location of stations [3]. On the other hand, there is limited number of real near-fault records all over the world such as Northridge 1994 and Kobe 1995. Hence, using synthetic records or simulated pulse-like records can be helpful to study the effects of near-source records on structures.

In general, forward-directivity near-fault records are simulated by pulse-like and simple models. Pulse period (T_p) and PGV are the most important parameters in pulse-like excitations [6]. In addition, decaying sinusoidal simulated record has shown better adaptation with real near-fault records among several models proposed by researchers [7].

In this process, seven real near-fault records are selected firstly. Later, the equivalent decaying sinusoidal record is made for each of selected real records. Steel moment resisting frames with different height are designed and modeled individually. IDA is used to investigate the performance of frames in a wide range from elasticity to dynamic instability. Finally, different types of IDA curves will be produced. On the one hand, PGA has been used as an intensity measure. On the other hand, although spectral acceleration (S_a) is currently the main intensity measure in estimation of seismic demand of SMRFs, some recent studies have shown that these IM may have not the same accuracy for estimating the seismic demand of all frames with different height [8-10]. They express that $S_a(T_1)$ is a better IM than PGA but is not an appropriate IM parameter for tall buildings, especially those subjected to near-fault ground motions. Hence, in this paper, PGV is selected as another IM parameter. Moreover, the relative drift of stories in various intensities of real and decaying sinusoidal records is obtained. Finally, sensitivity is assessed for changes in parameters of decaying sinusoidal record, pulse frequency (ζ_p) and damping ratio (ω_p).

According to the fact that an important issue in performance-based earthquake engineering is the estimation of structural performance under seismic loads, an appropriate method that has recently used to calculate a certain limit-state capacity is IDA [1]. Hence, in this study, performance criteria introduced in FEMA-350 [11] are estimated and also compared through all frames subjected to real and decaying sinusoidal records.

2. Literature Review

A great number of researches have been carried out about near-field ground motions and pulse-like simulated records. The forward-directivity near-fault records, were simplified by several pulse-like models such as P1, P2, P2,1 and P2,2 by Alavi and Krawinkler in 1998 [12]. In addition, Markis et al. [3] proposed A, B and C_n models to simplify near-fault pulses. Agrawal et al. [7] proposed decaying sinusoidal record as a proper alternative for pulse-like near-source records in 2002. Trica et al. [5] investigated pulse-like models on steel moment resisting frames in 2003. They focused on changes in responses and ductility. Markis and Black [13] investigated the advantages of PGV as an intensity measure for pulse-like ground motions in 2004. They also compared pulses in acceleration records with pulses in velocity records. Shakib and Hashemi [6] in 2006, compared real, synthetic and equivalent pulse-like ground motion records for north Tehran fault. Sehhati et al. [14] focused on the structural responses of multi-story structures to near-fault ground motions, and whether structural responses is dominated by the ground motion pulses present in

forward-directivity ground motions in 2011. They also considered whether simplified pulses are capable of representing the effects of these pulses on structural responses. They employed incremental dynamic analysis to assess the effects of forward-directivity pulses on the responses of near-fault multi-story structures.

On the other hand, the initial idea for incremental dynamic analysis refers to Bertero [15]. Since 2000, Cornell and Vamvatsikos have employed IDA in many researches. In 2002, they published a paper on incremental dynamic analysis [1-2]. In this paper, definitions choose a suitable intensity measure and an algorithm for IDA method was explained. During the last decade, IDA is accepted by FEMA as a suitable method to define limit states and capacity in structures [11]. In 2003, Vamvatsikos et al. [16] employed IDA on an RC-structure. Oesterle used IDA to assess the performance of steel moment-resisting frames with fluid viscous dampers in 2003 [17]. In 2006, Vamvatsikos employed IDA to evaluate the seismic performance of a 20-story steel frame [18]. In this study, IDA curve was generalized to three-dimensional space. Asgarian et al. [19] performed Comparative studies on the seismic performance of three different types of steel moment-resisting frames in 2009. Analytical models of connections were employed including panel zone and beam to column joint model. Incremental dynamic analysis was then utilized to assess the structural dynamic behavior of the frames and to generate required data for performance based evaluations. In 2012, Cheraghi Afarani et al. [20] applied IDA to estimate response of stiffness irregular structures to seismic loads. By comparison of expected collapse capacity of maximum considered earthquake and stiffness irregular structures, collapse safety was evaluated. Stiffness irregularity in lower stories has more effects on response of structure than intermediate stories and leads to lower collapse safety.

3. Ground Motion Records

In this study, seven forward-directivity real near-fault ground motion records are selected, Table (1) [21]. They are all related to fault normal component, and the selected records contain fault mechanism similar to north Tehran fault and soil type is similar to the site in the northern Tehran.

4. The Process of Simulating Real Records by Decaying Sinusoidal Record

As mentioned before, among various simulated and simplified models for near-fault pulse-like excitations, decaying sinusoidal record has shown better adjustment with real near-fault pulse-like records. This simulated model was proposed by Agrawal et al. [7] and is able to simplify pulse properties of velocity time history by a decaying sinusoidal function. The velocity time history of the resulting function expressed as:

$$\dot{u}_g = s \times e^{-\varsigma_p \omega_p t} \sin(\omega_p \sqrt{1-\varsigma_p^2}\, t) \tag{1}$$

The resulting acceleration time history obtains as the following function:

$$\ddot{u}_g = s \times e^{-t\varsigma_p \omega_p} [(-\varsigma_p \omega_p] \sin(\omega_p \sqrt{1-\varsigma_p^2}\, t) + (\omega_p \sqrt{1-\varsigma_p^2}) \cos(\omega_p \sqrt{1-\varsigma_p^2}\, t)] \tag{2}$$

Table 1. The suite of seven real near-fault ground motion records [21].

NO	Event	Station	M_w[1]	R[2](km)	M[3]	V_s[4] (m/s)	D[5] (km)	E_D[6] (km)	H_D[7] (km)	PGA (g)	PGV (cm/s)
1	Coalinga 1983	1651-Transmitter	5.8	9.2	R[8]	360-750	7.4	5.99	9.52	0.84	44.1
2	Northridge1994	24207-Pacoima Dam	6.7	8	R	360-750	17.5	20.36	26.85	1.28	103.9
3	Cape Mendocino 1992	89156-Petrolia	7.1	9.5	R	360-750	9.6	4.51	10.52	0.66	89.7
4	Northridge1994	00000-LA Dam	6.7	2.6	R	360-750	17.5	11.79	21.10	0.51	63.7
5	Northridge1994	77-Rinaldi	6.7	7.1	R	360-750	17.5	10.91	20.62	0.83	166.1
6	San Fernando1971	279-Pacoima Dam	6.6	2.8	R	360-750	13	11.86	17.6	1.226	112.5
7	Whittier Narrows1987	90019-San Gabriel	6	9	R	360-750	14.6	4.77	15.36	0.304	23

1. Moment Magnitude
2. Closest distance to the fault plane
3.Fault Mechanism
4. Shear wave velocity in the soil
5. Depth
6. Epicentral Distance
7. Hypocentral Distance
8. Reverse

In Eqs. (1) and (2), ς_p, ω_p and $s \times e^{-\varsigma_p \frac{\pi}{2\sqrt{1-\varsigma_p^2}}}$ respectively, are the damping ratio, pulse frequency and the maximum amplitude of the velocity time history. To simplify real records by decaying sinu-soidal model, the parameter of ς_p, ω_p and s are selected so that there is an appropriate adjustment in the velocity time history related to real and decaying sinusoidal record. Due to the fact that in many equations, pulse period is used more than frequency as well as PGV is used instead of s, the following equations can be mentioned:

$$T_p = \frac{2\pi}{\omega_p} \tag{3}$$

$$PGV = s \times e^{-\varsigma_p \frac{\pi}{2\sqrt{1-\varsigma_p^2}}} \tag{4}$$

On the other hand, Marek and Rodreguez proposed Eq. (5) in 2000 [6] based on 48 near-fault sample records with moment magnitude (M_w) in a range of 6.1-7.4 is the most logical to calculate PGV. Hence, it is employed to estimate PGV in simulated decaying sinusoidal record in the current study.

$$Ln(PGV) = 2.44 + 0.5M_w - 0.41\,Ln(r^2 + 3.93^2) \tag{5}$$

where M_w is the moment magnitude and r is the fault distance in km. In addition, the normal forward-directivity component to the fault plane is employed to estimate pulse period. Finally, the following equation has been proposed by Shakib and Hashemi [6] based on the condition of north Tehran fault and other faults caused by a similar mechanism.

$$Log_{10}^{T_p} = -2.1934 + 0.3431M_w \tag{6}$$

In order to provide decaying sinusoidal simulated records, the parameter of ς_p is required. In this paper, ς_p = 0.1, 0.2 is used to make equivalent decaying sinusoidal records. It is noted that the dependence of responses to ς_p will be discussed.

Table (2), indicates required parameters as well as the values of PGA and PGV in decaying sinusoidal records equivalent with real ground motion records introduced in Table (1). As a sample, velocity time histories of the two selected real and decaying sinusoidal records are presented in Figure (1).

5. Design of Structures

To evaluate the performance of SMRFs subjected to real near-fault records and equivalent decaying sinusoidal records, three steel moment-resisting frames are considered. The buildings are five, ten and fifteen stories high and are designed as regular structures for a site (Tehran, Iran), which represent high seismic zone. These buildings assumed to be located on soil type B (average shear wave velocity to a depth of 30 m would be 360-750 m/s) and with close distance to the north Tehran fault. The buildings are square in plan and consist of two bays of 4.0 m in each direction and the story heights of buildings are 3.0 m, Figures (2) and (3).

A rigid diaphragm can be assumed according to the roof system existing in usual structures. Gravity loads are supposed to be similar to common residential buildings in Iran [22]. Seismic loading is done based on the Iranian Seismic Code 2800 [23]. Details of the building in the strong direction are irrelevant in this study because the structures are only loaded along their weak axis. IPE and HEB sections are used to design beams and columns, respectively. Fundamental period of designed 5, 10 and 15-story buildings are 0.7 s, 1.2 s and 2.6 s, respectively.

Table 2. equivalent decaying sinusoidal simulated records.

No	Event	Station	*Tp*	*S*	ς_p	ω_p	PGA (cm/s^2)	PGV (cm/s)
1	Coalinga 1983	1651-Transmitter	0.62	65	0.1	10	718	55
2	Northridge1994	24207-Pacoima Dam	1	144	0.2	6.3	1260	105
3	Cape Mendocino 1992	89156-Petrolia	1.96	124	0.2	3.2	650	90
4	Northridge1994	00000-LA Dam	1.31	98	0.2	4.8	554	70
5	Northridge1994	77-Rinaldi	1.2	226	0.2	5.2	822	166.1
6	San Fernando1971	279-Pacoima Dam	1.31	142	0.2	4.8	1205	112
7	Whittier Narrows1987	90019-San Gabriel	0.78	30	0.1	8	298	23

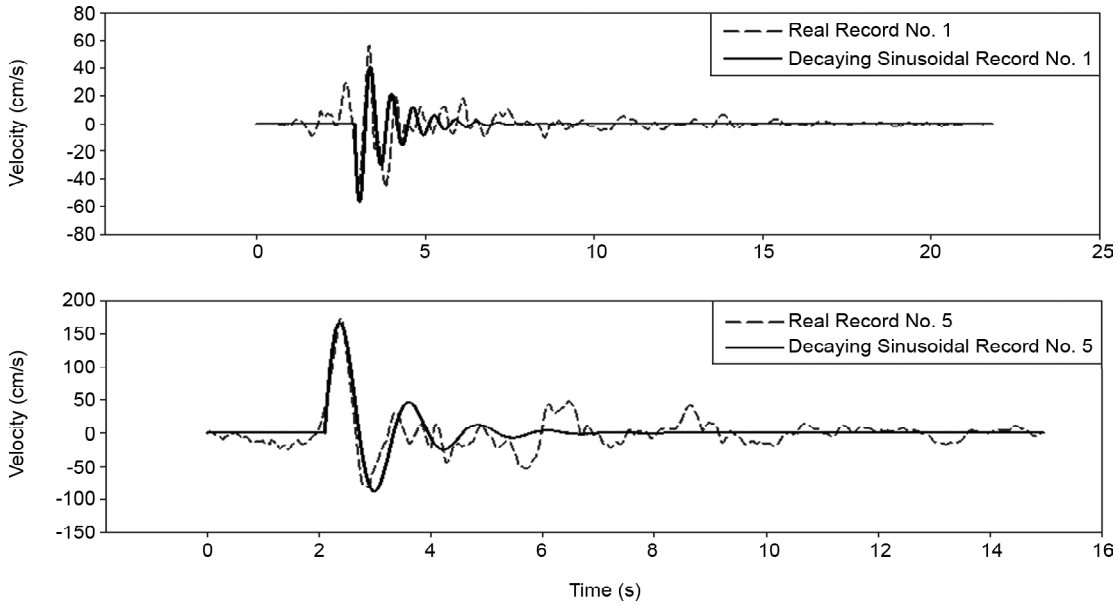

Figure 1. Velocity time histories of the real and equivalent decaying sinusoidal records No. 1 and 5.

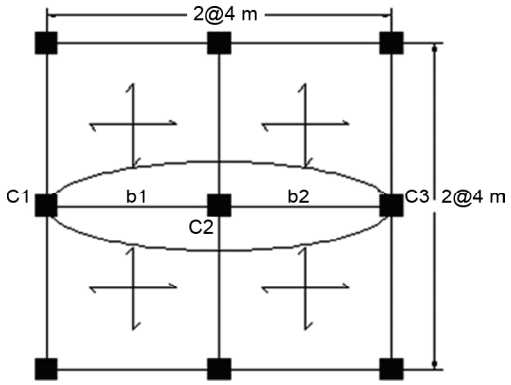

Figure 2. Typical plan view of buildings.

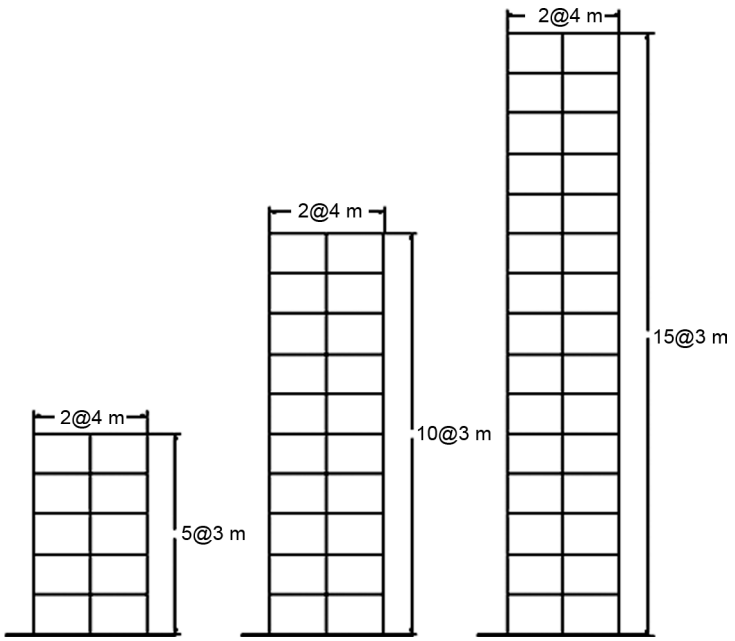

Figure 3. Geometry of the frames.

6. Numerical Modeling

To perform IDA, frames are modeled in SeismoStruct-V5 [24] finite element software that is able to perform nonlinear dynamic analysis. To model the steel behavior, bilinear kinematic stress-strain curve is assigned to the elements from the library of materials introduced in SeismoStruct. In addition, distributed inelasticity elements are widely employed in earthquake engineering applications, either for research or professional engineering purposes. It is simply noted that distributed inelasticity elements do not require calibration of empirical response parameters against the response of an actual or ideal frame element under idealized loading conditions, as is instead needed for concentrated-plasticity phenomenological models.

Distributed inelasticity frame elements can be implemented with two different finite elements (FE) formulations: the classical displacement-based (DB) ones [24-25] and the force-based (FB) formulations [24, 26]. In SeismoStruct, it is mentioned that FB formulation is always exact and has more accuracy than DB formulation. On the other hand, inelastic plastic hinge frame element (infrmFBPH: Inelastic Frame Elements Force Base Plastic Hinge) is the plastic-hinge counterpart to the FB element, featuring a similar distributed inelasticity forced-based formulation, but concentrates such inelasticity within a fixed length of the element. The number of section fibres used in equilibrium computations carried out at the element's end sections needs to be defined. The ideal number of section fibres, sufficient to guarantee an adequate reproduction of the stress-strain distribution across the element's cross-section, varies with the shape and material characteristics of the latter, depending also on the degree of inelasticity to which the element will be forced to [24]. In this study, infrmFBPH is used in modelling the element of beams and columns, and the number of section fibres is 200 for both beam and column elements. Besides, Hilber-Hughes-Taylor integration scheme is used for time integration. Geometric non-linearity, which can have a significant role in the response of near-fault structures, is also considered.

7. Performing IDA and Analysis Results

IDA are performed for each of the three structures using the input ground motions listed in Tables (1) and (2) (real near-fault records and equivalent decaying sinusoidal records, respectively). Only the fault normal component of each record is applied to the structures and it is assumed that the weak axes of the structures are perpendicular to the fault [14]. Once, PGA is selected as an intensity measure. Because of the presence of pulse period in velocity records that has a significant role in responses [14], PGV is selected as another intensity measure in this study. Finally, the adaptation of responses under the real and simulated records is measured once for PGA as an intensity measure and once for PGV as another intensity measure. To perform the actual nonlinear dynamic analyses required for IDA, each record is scaled to cover the entire range of structural response, from elasticity to yielding, and finally collapse. A linear time history analysis is performed first to establish an elastic baseline. Next, a nonlinear time history analysis is performed and the maximum inter-story drift value is obtained. The ground motion is then incrementally increased and the analysis repeated until numerical non-convergence is encountered [19]. Different types of IDA curve and responses are produced: PGA-θ_{max}, PGV- θ_{max}, PGV-maximum base shear, dynamic push-over curves, inter-story drift ratio in different intensities, the evaluation of structural performance subjected to real and decaying sinusoidal records. More details will be provided on each of the IDA curves and other responses individually. In all charts, *R* and DS are representative Real and Decaying Sinusoidal records, respectively.

7.1. IDA Curve (PGA- θ_{max} *)*

In the first IDA curve that is interpreted, PGA is selected as IM and maximum inter-story drift ratio (θ_{max}) is selected as DM. The results of this IDA curve for the frames subjected to the real and the equivalent decaying sinusoidal records are shown in Figure (4). Observations show a proper adaption between both groups of curves since the approximate intensity of 1 g for all frames. After the former approximate intensity, the IDA curves related to real and decaying sinusoidal records are somewhat different due to the differences in PGA of real and equivalent simulated records. Finally, about the intensities that lead to global instability, differences will be greater. Observe that the mean structural response to the real records is almost equal to the equivalent decaying sinusoidal records in low

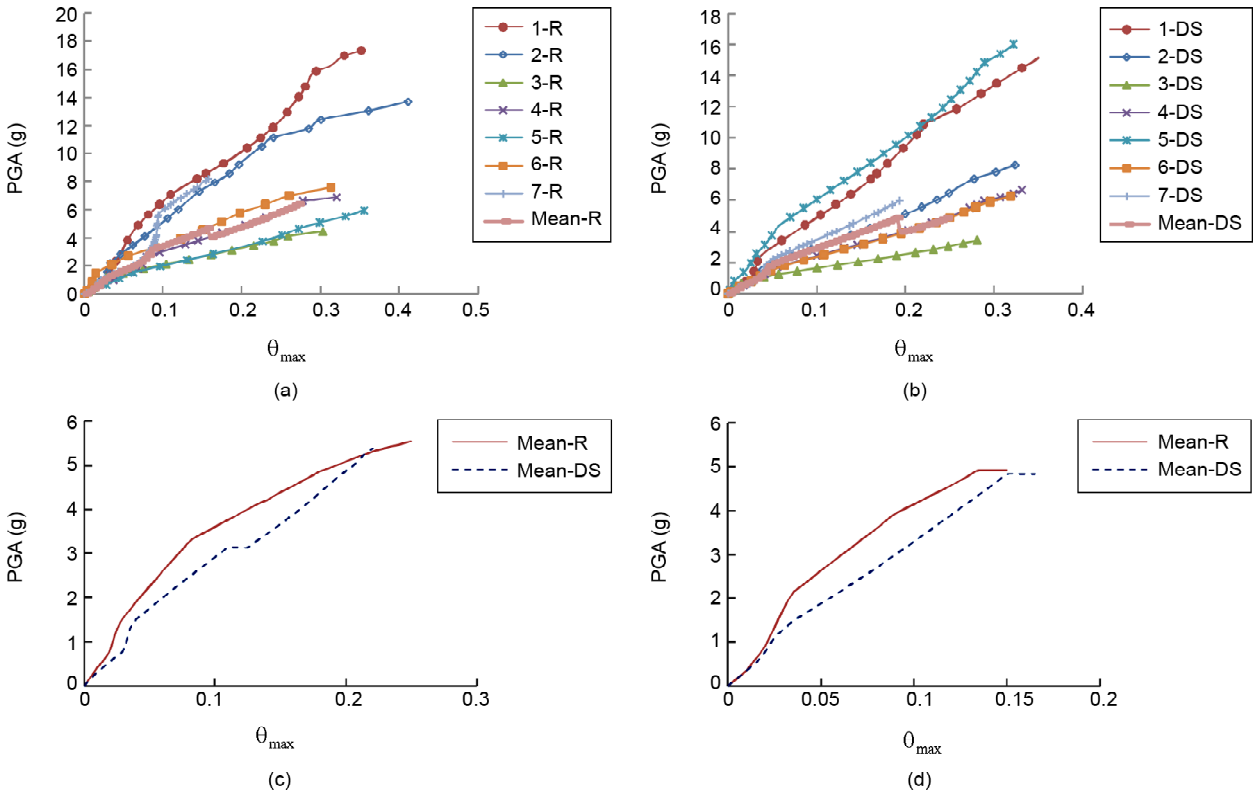

Figure 4. IDA curve (PGA-θ_{max}) for a) 5-story frame subjected to the 7 real records; b) 5-story frame subjected to the 7 decaying sinusoidal records; c) the mean curves for 10-story frame; d) the mean curves for15-story frame.

intensities but gradually different for high intensities. Overall, for low intensities, the average differences in the mean PGA-θ_{max} curve for 5, 10 and 15 story frames subjected to the real and decaying sinusoidal records approximately fall in a range of 10% to 20%, and for high intensities, fall in a range of 20% to 30%.

Moreover, the scattering of responses are significant in this type of IDA curve. It is observed that the dispersion of responses is high while PGA is used as intensity measure for IDA curves.

7.2. IDA Curve (PGV-q_{max})

Because of the presence of initial velocity pulse, PGV is selected as another intensity measure. In this process, for each of the real and simulated records PGV is scaled to a wide range from low to high values. Then the corresponding acceleration time history per PGV are achieved and applied to the frames. Hence, IDA curves based on the changes in the peak ground velocity is produced. The results of this IDA curve for the frames subjected to real and the equivalent decaying sinusoidal records are shown in Figure (5).

Observations in Figure (5) (PGV-θ_{max}) show good adaption with much lower differences between IDA curves related to the real and to the equivalent decaying sinusoidal records in comparison with Figure (4) (PGA-θ_{max}). For low intensities, the average differences in the mean PGV-θ_{max} curve for 5, 10 and 15 story frames subjected to the real and the decaying sinusoidal records is approximately lower than 10% and for high intensities, fall in an approximate range of 10% to 15%. Hence, it is clear that in low intensities, there is a good adaption between structural responses under real and equivalent decaying sinusoidal records. However, by intensifying the excitations, the differences are enhanced.

Another important point in this type of IDA curve is the much lower dispersion of responses. Surprisingly, IDA curves for equivalent decaying sinusoidal records are denser especially when PGV is used as intensity measure. The maximum standard deviation (θ_{max}) of the PGV-θ_{max} curves for all frames are calculated in a range of applied peak ground velocity from 100cm/s to 800cm/s and shown in Table (3). It is clear that θ_{max} for the decaying sinusoidal records in all frames falls in a smaller range compared with the real records. In brief, the structural responses for all frames show lower scatter while PGV is the intensity measure. Moreover, the dis-

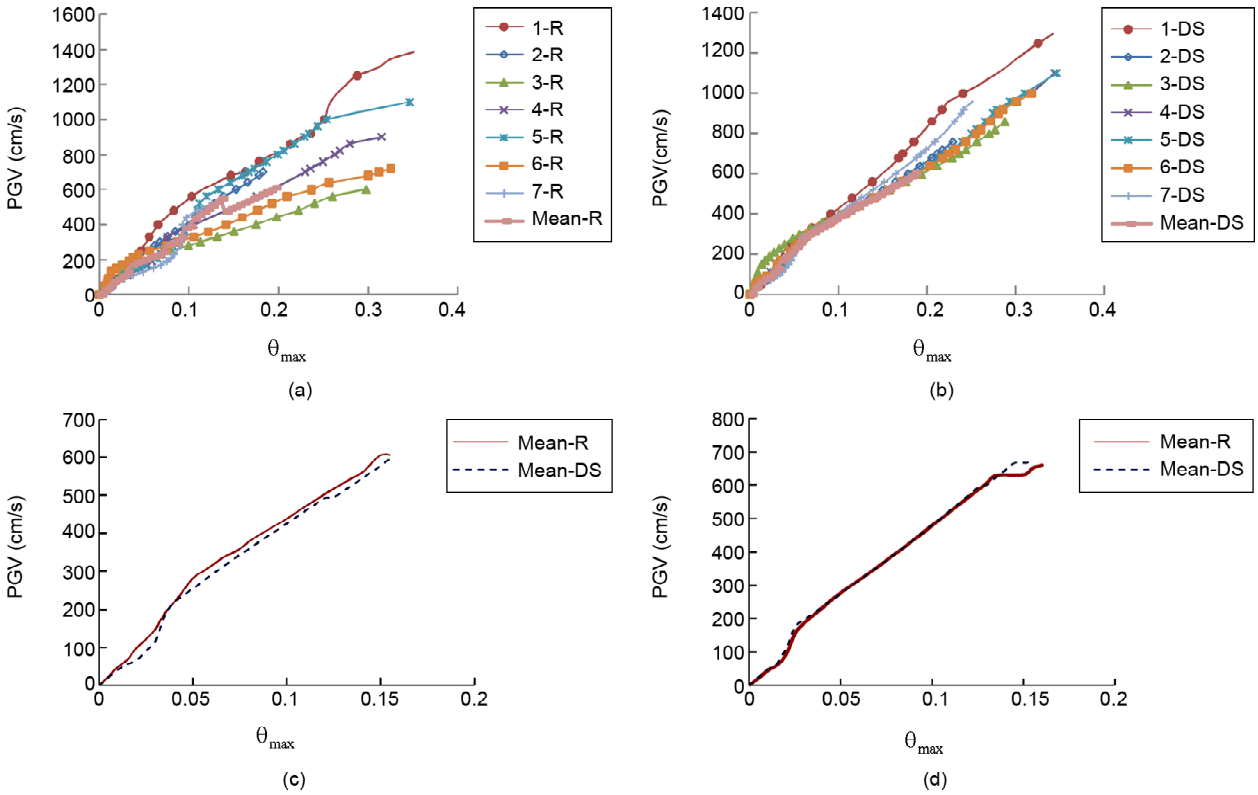

Figure 5. IDA curve (PGV-θ_{max}) for a) 5-story frame subjected to the 7 real records; b) 5-story frame subjected to the 7 decaying sinusoidal records; c) the mean curves for 10-story frame; d) the mean curves for15-story frame.

Table 3. The range of σ_{max} in PGV- θ_{max} curves for a range of applied velocity(100 cm/s - 800 cm/s).

	5-Story Structure	10-Story Structure	15-Story Structure
Real Records	(0.2-2)%	(0.07-2)%	(0.09-1.8)%
Equivalent Decaying Sinusoidal Records	(0.2-1.1)%	(0.15-1.1)%	(0.14-0.83)%

persion in structural responses to the decaying sinusoidal records is much lower according to the Figure (5) and Table (3).

7.3. IDA Curve (PGV-Maximum Base Shear)

In this type of IDA curve, PGV is selected as the intensity measure and the corresponding maximum base shear that has created in the structures is selected as damage measure. The curves are shown in Figure (6). For all frames, there is a similar process depicted in figures since the approximate maximum base shear 600 KN. Then, there is a gradual trend through going up. Similar to pervious IDA curves, there is a good adaption between curve related to the real and decaying sinusoidal records in low intensities and dispersion is increased by intensifying excitations. For low intensities, the average differences in the mean PGV-maximum base shear curves for 5, 10 and 15-story frames subjected to the real and the decaying sinusoidal records is approximately lower than 5% and for higher intensities, fall in a range of 10% to 15%. Finally by increasing the intensities, the differences become more.

7.4. Dynamic Push-Over Curves

One of the most important curves in dynamic analysis is the dynamic push-over curve. The process to achieve this curve is almost similar to static push-over curve. There is much more information that we could easily glean out of the IDA by taking a closer look at the results and plotting them in new ways [2]. Simply, in each step of IDA in which the input record enlarged, the sum up maximum base shear and top displacement are calculated and make up discrete points. By linking these points together, the dynamic push-over curve is obtained for each record. In this study, dynamic push-over curves are shown in Figure (7). In each step, the input PGV is

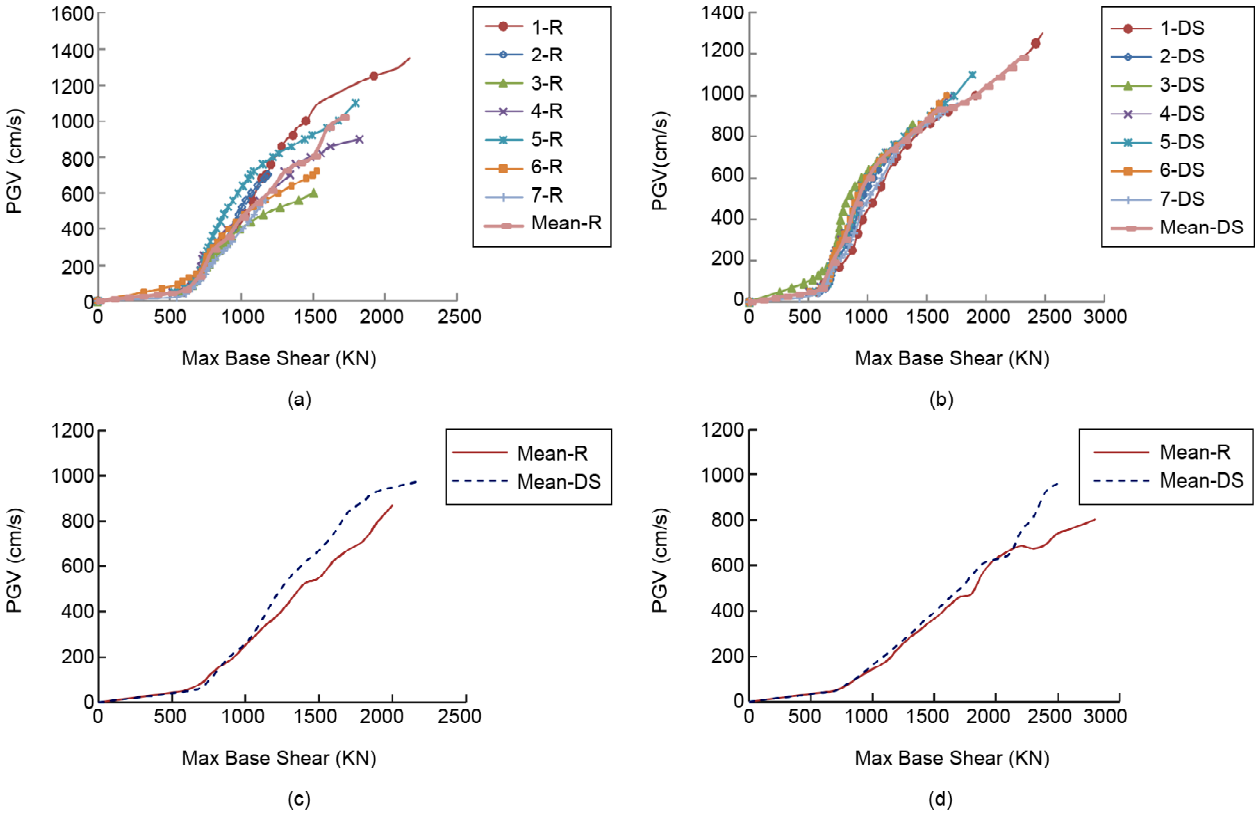

Figure 6. IDA curve (PGV-maximum base shear) for a) 5-story frame subjected to the 7 real records; b) 5-story frame subjected to the 7 decaying sinusoidal records; c) the mean curves for10-story frame; d) the mean curves for15-story frame.

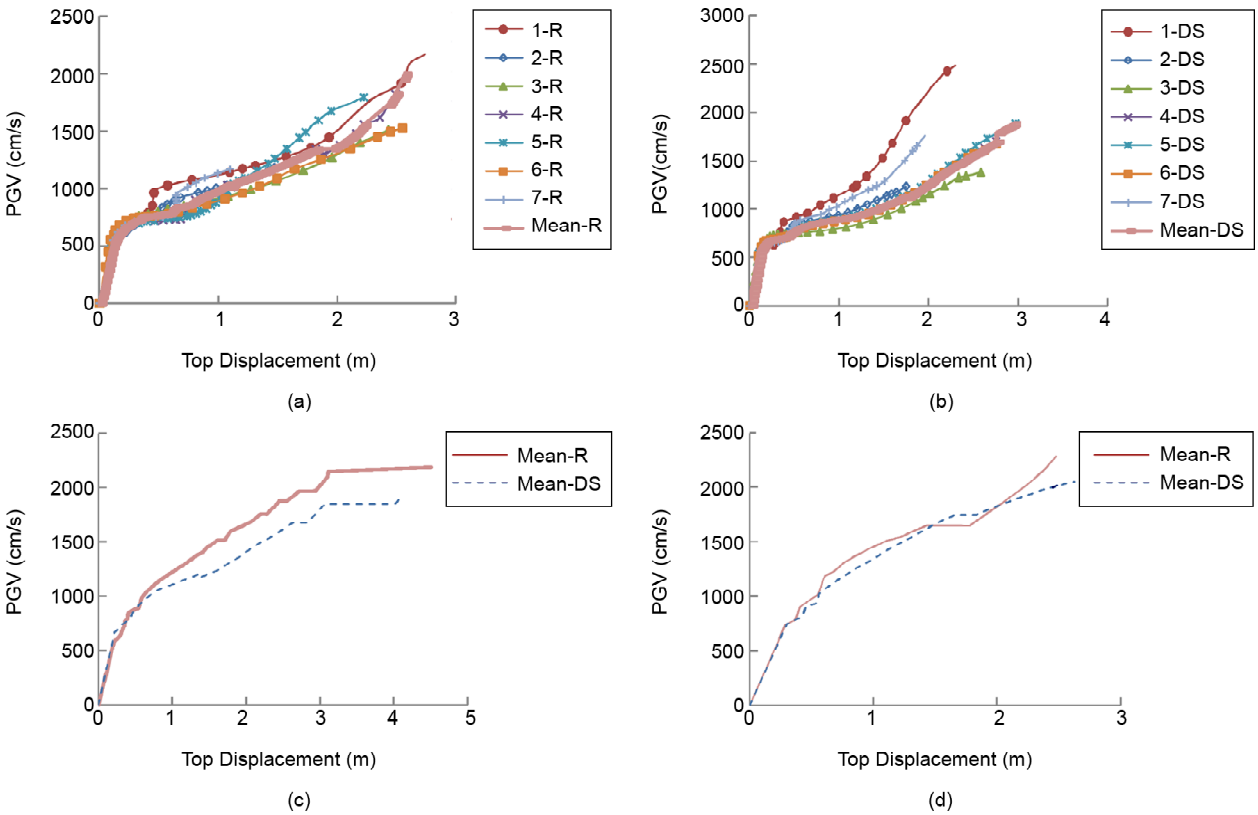

Figure 7. Dynamic push-over curves for a) 5-story frame subjected to the 7 real records; b) 5-story frame subjected to the 7 decaying sinusoidal records; c) the mean curves for10-story frame; d) the mean curves for15-story frame.

scaled up and the corresponding maximum base shear and top displacement is gained as discrete points and by linking them together, the dynamic push-over curve is obtained. Similar to what happened in the previous charts, the differences in dynamic push-over curves for all frames subjected to the real and decaying sinusoidal records in the low intensity of excitations are lower than high intensities. In low intensities, the average differences are lower than 5%, and for higher intensities it falls in a range of 5% to 15%.

8. Performance Evaluations

In this study, seismic performance evaluation procedures involve the estimation of a level of confidence that a structure will be able to achieve a desired performance objective as outlined in FEMA-350 [11]. One way to study seismic performance is to perform IDA and define limit-states on IDA curves.

8.1. Defining Limit-States on IDA Curves

Based on FEMA-350, three commonly used limit states are considered namely Immediate Occupancy (IO), Collapse Prevention (CP) and Global Dynamic Instability (GI) are chosen [11]. This study has focused on IO and CP limit states and has calculated them according to FEMA-350 guidelines [11]. Related damages to structural components of these limit states are as follows:

IO: Minor local yielding at a few places without permanent distortion of members.

CP: Extensive distortion of beams and column panels. Many fractures at moment connections without shear connection failure [11, 20].

The IO limit-state is defined at θ_{max} = 2% and for the CP limit-state two criteria are to be met. Collapse prevention is not exceeded on the IDA curve until the final point where the local tangent reaches 20% of the elastic slope or θ_{max} = 10%, whichever occurs first in IM terms [1].

8.2. Summarizing the IDAs

By generating the IDA curve for each record and subsequently defining the limit-state capacities, large amount of data can be gathered, Figures (4) and (5). As observed, the range of behavior that the IDA curves display shows large record-to-record variability. Hence, it is essential to summarize such data and quantify the randomness introduced by the records. It is needed to employ appropriate summarization techniques that will reduce this data into the distribution of DM given IM and the probability of exceeding any specific limit-state given the IM level [1].

There are several methods to summarize the IDA curves, but the cross-sectional fractile is arguably the most flexible [1].

The limit-state capacities can be easily summarized into some central value (e.g., the median) and a measure of dispersion (e.g., the standard deviation). Consequently, it has been chosen to calculate the 16%, 50% and 84% fractile values of DM and IM capacity for each limit-state [1, 19].

In this study, summarized IDA curves for 5, 10 and 15-story frames subjected to the real and decaying sinusoidal records with PGA as the IM are shown in Figure (8), respectively. Besides, summarized IDA curves for aforementioned frames with PGV as intensity measure are shown in Figure (9). Limit state capacities (IO, CP) for the frames are listed in Table (4) and (5). Moreover, CP limit states

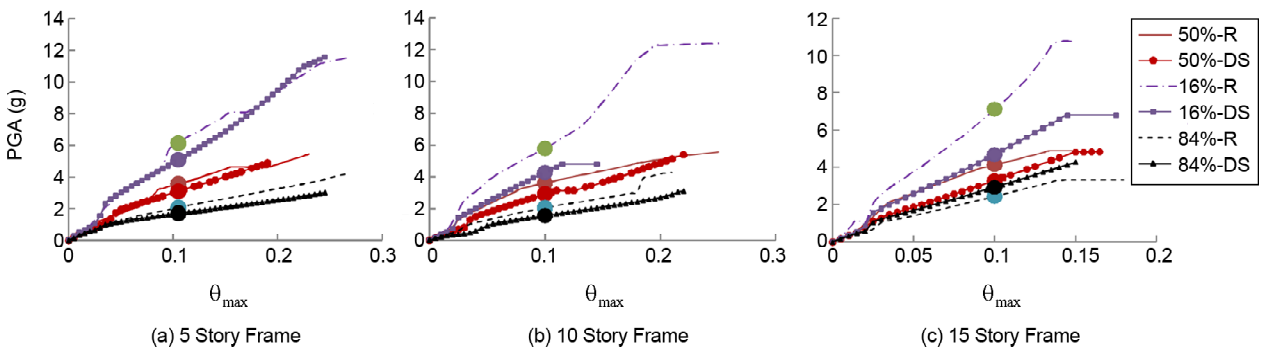

Figure 8. The summary of the IDA curves (PGA - θ_{max}) into their 16%, 50% and 84% fractile curves for the frames subjected to the real and equivalent decaying sinusoidal records.

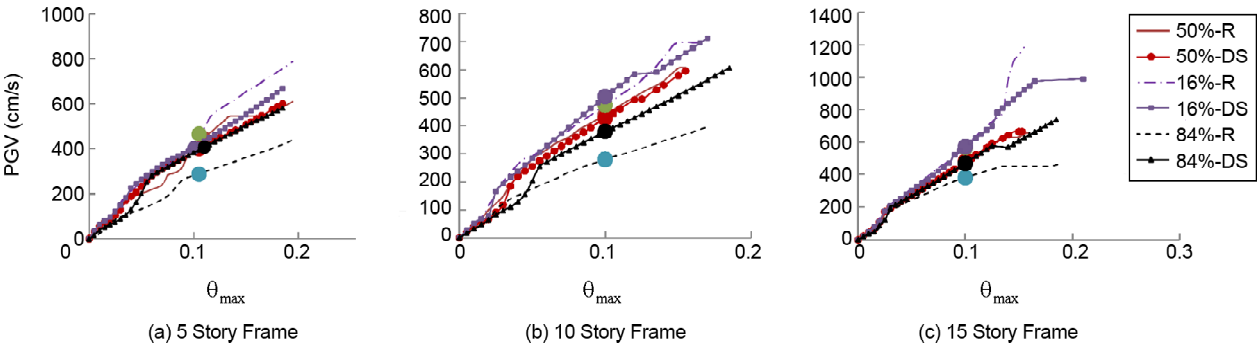

Figure 9. The summary of the IDA curves (PGV - θ_{max}) into their 16%, 50% and 84% fractile curves for the frames subjected to the real and equivalent decaying sinusoidal records.

Table 4. Summarized capacities for each limit-state on IDA curves (PGA- θ_{max}).

	5-Story Frame				10-Story Frame				15-Story Frame			
	Real Records		Decaying Sinusoidal Records		Real Records		Decaying Sinusoidal Records		Real Records		Decaying Sinusoidal Records	
	IO	CP	IO	CP	IO	CP	IO	CP	IO	CP	IO	CP
16%	0.93g	5.94g	0.82g	4.92g	1.15g	5.78g	0.74g	4.28g	0.98g	7.13g	0.87g	4.70g
50%	0.85g	3.48g	0.66g	2.99g	0.84g	3.60g	0.56g	2.90g	0.91g	4.14g	0.78g	3.29g
84%	0.47g	2g	0.57g	1.66g	0.49g	2.05g	0.33g	1.55g	0.57g	2.44g	0.58g	2.93g

Table 5. Summarized capacities for each limit-state on IDA curves (PGV- θ_{max}).

	5-Story Frame				10-Story Frame				15-Story Frame			
	Real Records		Decaying Sinusoidal Records		Real Records		Decaying Sinusoidal Records		Real Records		Decaying Sinusoidal Records	
	IO	CP	IO	CP	IO	CP	IO	CP	IO	CP	IO	CP
16%	89.57	449.46	96.91	403.60	113.11	473	76.66	503.44	130.79	568.49	111.90	572.79
50%	85.68	388.27	86.06	387.13	99.17	438.51	66.25	426.05	92.21	479.15	109.68	479.66
84%	70.78	280.67	63.03	382.76	62.06	278.84	63.13	377.40	74.01	382.35	86.80	469.91

are depicted on summarized curves as dots.

By qualitative and quantitative investigating performance levels of frames on summarized IDA curves according to Figure (8) and Table (4), differences are observed in these limit states in all frames subjected to the real records and the equivalent decaying sinusoidal records. For instance, the differences at IO limit state in 5 and 15-story frames are much lower compared with 10-story frames. Overall, it can be said that approximately the differences in IO limit state for 5, 10 and 15-story frames fall in a range of 10%-20%, 30%-35% and 10%-15%, respectively. On the other hand, for CP limit state, the corresponding differences for aforementioned frames subjected to the real and simulated records are almost 14%-17% for 5-story frame, 20%-25% and 20%-30% for 10 and 15-story frames, respectively.

In addition, in the majority of summarized IDA curves in all frames, performance levels of IO and CP related to decaying sinusoidal records are less than real records. Hence, it can be concluded that the seismic performance of frames subjected to decaying sinusoidal records is more conservative than real records and performance levels obtained in lower intensities of excitation in frames subjected to this simulated record.

According to Figure (9) and Table (5) and with similar look, observe that the differences are less while PGV is the IM of IDA curves. It can be said that approximately the differences at IO limit state for 5, 10 and 15-story frames are less than 10%, 30% and almost 15%, respectively. Moreover, the differences at CP in all frames subjected to the real records and simulated ones are almost less than 10%. Nevertheless, the same conclusion can be obtained.

In other words, in the majority of summarized IDA curves for all frames, performance levels of IO and CP related to the decaying sinusoidal records are less than real records, and seismic performance of frames subjected to the decaying sinusoidal records is more conservative than real records.

9. Lateral Story Drift Investigation

According to the fact that the existing pulse period in near-source records has a significant effect on responses of buildings, relative story drift in several intensities of applied selected records are chosen to study this effect.

In order to investigate the lateral drift of stories subjected to the real and the corresponding decaying sinusoidal records in this study, the ratio of relative drift of story over the story height is used. Moreover, since the records in this paper are scaled based on PGA and PGV, lateral drifts are obtained in different intensities of PGA and PGV. In other words, among different time history analysis with several intensities that constitute IDA, some of them are chosen and the relative lateral story drift subjected to the records are calculated. The samples of relative lateral drift of stories in different intensities of PGA and PGV for 5, 10 and 15-story frames are shown in Figures (10) to (12), respectively. For all frames, proper adaptation is observed between responses to the real and decaying sinusoidal records while PGV is used as intensity measures. However, with PGA as the intensity measure, differences are clearly much more. Moreover, responses are strongly high for elementary floors. In other words, because of the existence of pulse period in velocity records, the first and second stories have the maximum relative drift, especially, in high intensities and the value of responses in last stories is negligible in comparison with those in elementary stories. It is also evident in Figure (13).

In Figure (13), the samples of individual story drift IDA curves are plotted for 5, 10 and 15-story frames, showing a record-specific picture of the

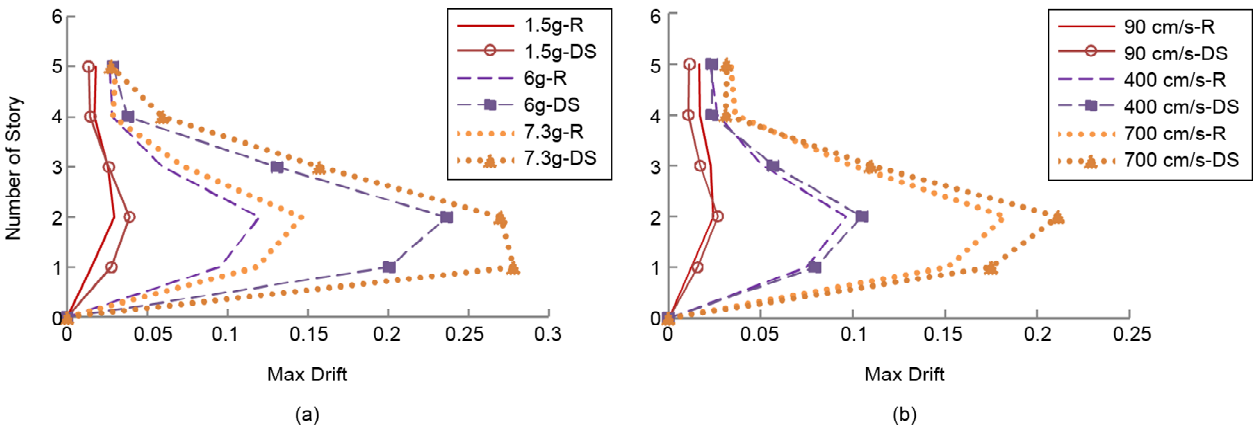

Figure 10. Lateral relative drift of 5-story frame subjected to record No. 2 in different intensities.

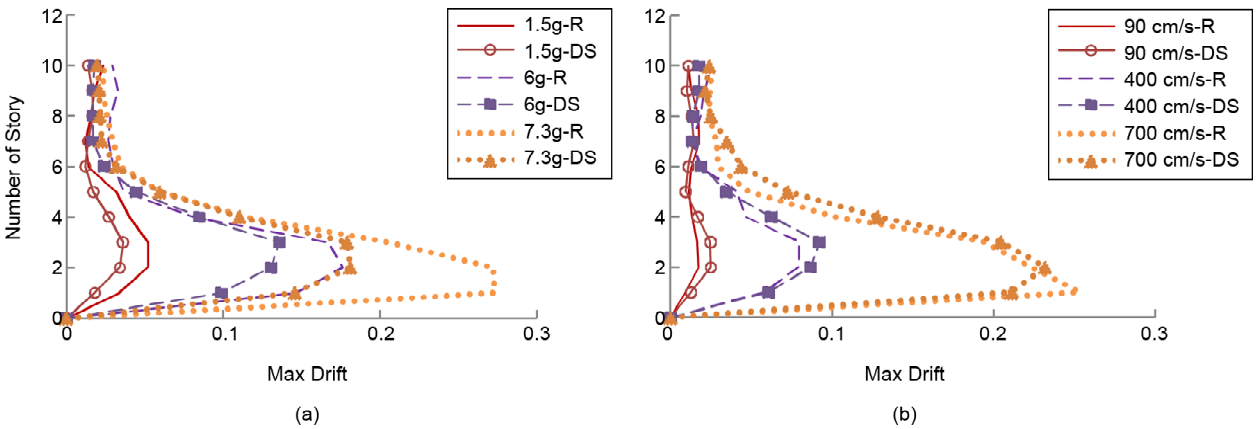

Figure 11. Lateral relative drift of 10-story frame subjected to record No. 5 in different intensities.

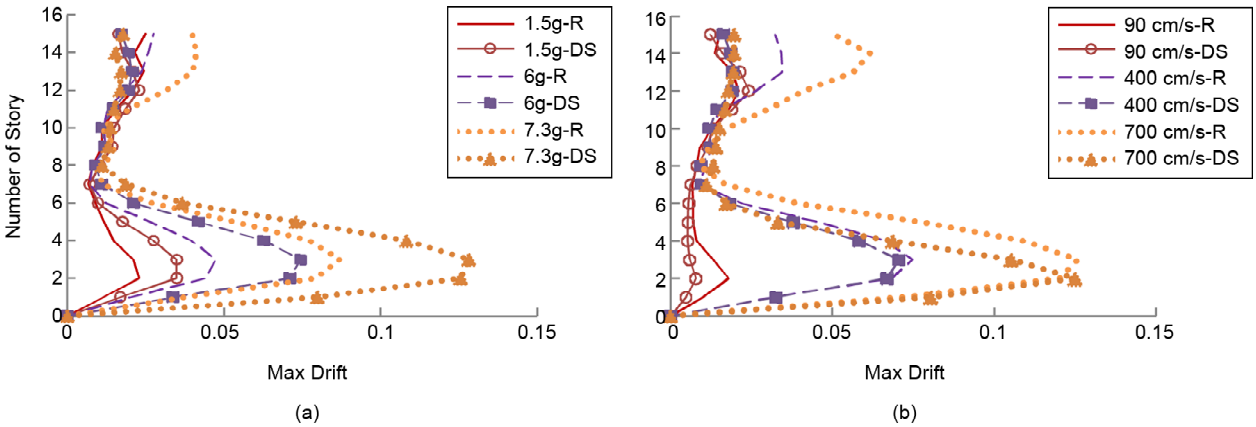

Figure 12. Lateral relative drift of 15-story frame subjected to record No. 7 in different intensities.

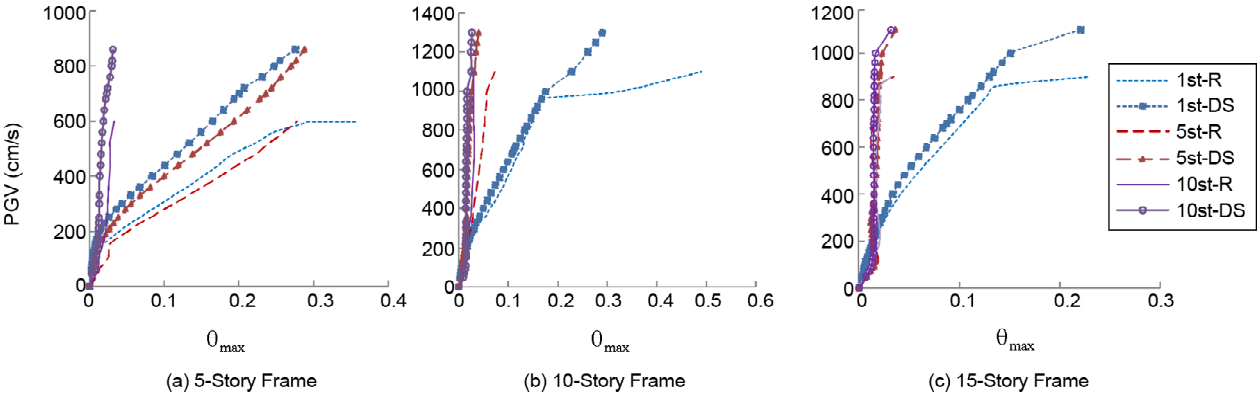

Figure 13. Samples of IDA curves separated story by story subjected to the records: a) No. 3; b) No. 1; c) No. 5.

elementary, middle and last-numbered floors. Most interesting is that for all frames subjected to the real near-fault ground motions listed in Table (1) and the equivalent decaying sinusoidal records listed in Table (2), elementary stories are experienced the most failure. In other words, base floors suddenly start accumulating progressive deformation as the IM increases. The pulse period in the beginning of forward directivity near-source records imposes a significant impact to the elementary stories. This pulse imposes severe demands to the structure. The arrival of the velocity pulse causes the elementary stories to dissipate considerable input energy [14]. Hence, the last stories contributions are less.

10. Discussion

The important parameters of simulated decaying sinusoidal records (pulse frequency and damping ratio) were obtained using relevant equations that described before. In order to investigate the structural responses to the modifications of afore-mentioned parameters, lateral relative story drift is selected. In this process, decaying sinusoidal records corresponding with selected real records, Tables (1) and (2), is reproduced using different values of pulse frequency while other parameters such as damping ratio are allocated to constant values. The range of changes in this parameter varies from lower values than pulse frequency equivalent with real record to higher amounts. A number of time history analyses are required to review lateral relative story drift of SMRFs subjected to decaying sinusoidal records with different pulse frequencies. A sample for studying the effect of variations in this parameter is depicted in Figure (14) for all frames subjected to record No. 1. It is obvious that the more the pulse frequency enhanced, the more the lateral relative story drift increased. For better explanation, base floors suddenly start accumulating progressive deformation as the pulse frequency increases. It is interesting that the pulse amplitude overshadowed by the pulse frequency since the elementary stories in all frames have the maximum relative drift. However, the values of

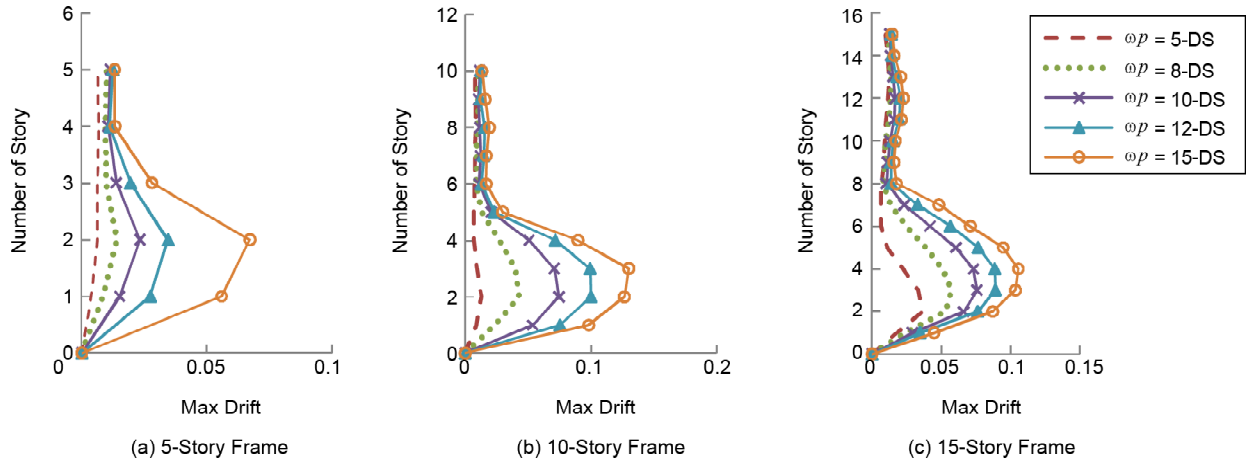

Figure 14. The effect of variations in pulse frequency parameter for Coalinga record, Transmitter station(ζ_p=0.1) on lateral story drift.

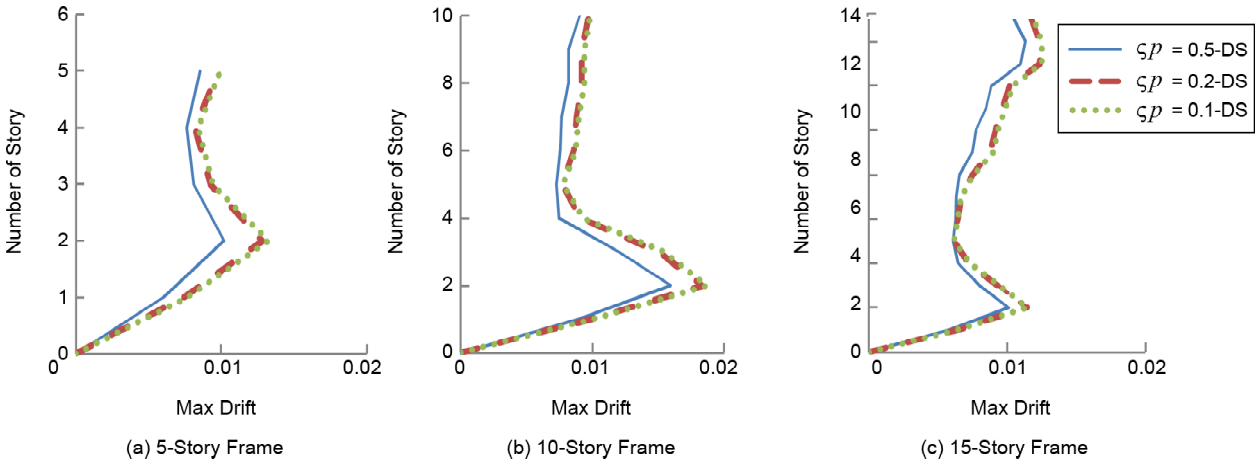

Figure 15. The effect of variations in damping ratio parameter forSan Fernando record,Pacoima Dam station on lateral story drift.

relative drift in last stories are negligible.

Moreover, the effects of variations in damping ratio of decaying sinusoidal record is studied on relative lateral story drift. As explained earlier, the decaying sinusoidal records equivalent with the real records are simulated using ςp = 0.1 and 0.2. Hence, it is worth to investigate the effect of this parameter on structural response. In this process, different damping ratio (ςp = 0.1, 0.2 and 0.5) in constant pulse frequency considered in order to investigate the effects of damping ratio on the response of the frames subjected to decaying sinusoidal records. In Figure (15), a sample for study variations of this parameter on lateral relative story drift in steel moment resisting-frames subjected to the decaying sinusoidal records No. 6 are shown. It is found that damping does not play a significant role in the response of frames. Especially, lateral relative story drift of frames subjected to records with ςp = 0.1 and 0.2 does not make much differences. Moreover, damping forces have little influence on frames subjected to pulse-like ground motions. This is because damping forces do not have sufficient time to dissipate the amount of impact and energy of pulse-like records imposed to the structure due to the short duration of the large-amplitude cycle.

11. Conclusions

In this paper, the structural responses of three steel moment-resisting frames with different height subjected to seven real near-fault pulse-like records and decaying sinusoidal records equivalent with those real ground motions have been investigated. In this regard, the equivalent simulated records have been made, IDA has been performed and different IDA curves were produced. Moreover, the seismic performance of frames has been evaluated by study on limit states under real and decaying sinusoidal records.

Finally, the effect of variations of significant parameters in decaying sinusoidal records on responses has been studied. It was shown that, in general, the simulated decaying sinusoidal record can be an ideal alternative for real pulse-like ground motions at low intensities of excitations. However, uncertainty is observed through responses at high intensities of excitations. Moreover, it was observed that most of summarized IDA curves and limit states (IO and CP) of frames subjected to decaying sinusoidal records are lower than real records. In other words, performance levels of IO and CP related to decaying sinusoidal records are less than real records and seismic performance of frames subjected to this simulated record is more conservative than real records.

It was also shown that for pulse-like ground motions, PGV is a more ideal IM than PGA and the dispersion in IDA curves, especially for frames subjected to decaying sinusoidal records is less while PGV is used as the intensity measure. In addition, the adaption between responses to the real and decaying sinusoidal records is more tangible while PGV is selected as the IM.

On the other hand, the pulse period in the beginning of forward directivity near-source records impose a significant impact to the elementary stories and make them experience the most deformations as it was clear in lateral drift of stories.

Pulse frequency is a significant parameter of decaying sinusoidal simulated records and it is obvious that the more the pulse frequency enhanced, the lateral relative story drift has increased more since this parameter effect on pulse amplitude.

Finally, it was shown that the parameter of damping ratio in decaying sinusoidal record does not play a significant role in the response of frames.

References

1. Vamvatsikos, D. and Cornell, C.A. (2002) The incremental dynamic analysis and its application to performance-based earthquake engineering, London. *Proceeding of 12th European Conf. of Engineering*, Paper Reference 479.

2. Vamvatsikos, D. and Cornell, C.A. (2002) Incremental dynamic analysis, *Earthquake Engineering and Structural Dynamics*, **31**(3), 491-514.

3. Somerville, P. (2000a) 'Characterization of near-fault ground motions'. In: *Effects of Nearfield Earthquake Shaking*, U.S.-Japan Workshop, San Francisco, 20-21 March, 21-29.

4. Somerville, P. (1998). *Development of an Improved Representation of Near Fault Ground Motions*. SMIP98 Seminar on Utilization of Strong-Motion Data, 1-20.

5. Trica, L.D., Foti, D., and Diaferio, M. (2003) Response of Middle-Rise Steel Frames with and without Passive Dampers to Near-Field Ground Motions, *Journal of Engineering Structures*, **25**(2), 169-179.

6. Shakib, H. and Hashemi, S.SH. (2006) Comparison and evaluation real, synthetic earthquake and near-fault equivalent pulse-like models, scientific-research. *J. of Omran-Moddares*. **10**(1), (In Persian).

7. Agrawal, A.K. and HE, W.L. (2002) A closed form approximation of near-fault ground motion pulses for flexible structures. *15th ASCE Engineering Mechanics Conference*, New York, Columbia University.

8. Mahdavi Adeli, M. and Banazadeh, M. (2011) Introducing a new intensity measure parameter for probabilistic seismic demand analysis of steel moment-resisting frames. *6th International Conference on Seismology and Earthquake Engineering*, Tehran, Iran.

9. Luco, N. and Cornell, C.A. (2007) Structure specific scalar intensity measure for near-source and ordinary earthquake ground motion. *Journal of Earthquake Spectra*, **23**(2), 357-392.

10. Baker, JW. and Cornell, C.A. (2008) Vector-valued intensity measures for pulse-like near-fault ground motions. *Journal of Engineering Structures*, **30**(4), 1048-1057.

11. SAC Joint Venture (2000) *Recommended Seismic Design Criteria for New Steel Moment-Frame Buildings*. Report No. FEMA-350, Prepared for the Federal Emergency Management Agency, Washington DC.

12. Alavi, B. and Krawinkler, H. (2002) *Effect of Near-fault Ground Motion on Frames Structures*. A Report on Research Sponsored by

National Science Foundation Grant CMS, California SMIP Contact No. 1079, 6.

13. Markis, N. and Black, C. (2004) Evaluation of peak ground velocity as a "Good" intensity measure for near-source ground motions. *Journal of Engineering Mechanic*s, **130**(9), 1032-1044.

14. Sehhati, R., Rodreguez, A., Elgawady, M., and Cofer, WF. (2011) Effect of near-fault ground motions and equivalent pulses on multi-story structures. *Journal of Engineering Structures*, **33**(3). 767-779.

15. Bertero, V. (2002) Performance-based seismic engineering: the need for a reliable conceptual comprehensive approach. *Journal of Earth quake Engineering and Structural Dynamics*. **31**(2), 627-652.

16. Vamvatsikos, D., Jalayer, F., and Cornell, C.A. (2003) Application of incremental dynamic analysis to an RC-structure. *Proceedings of the FIB Symposium on Concrete Structures in Seismic Regions*, Athens, Greece.

17. Oesterle, GM. (2003) *Use of Incremental Dynamic Analysis to Assess the Performance of Steel Moment-resisting Frames with Fluid Viscous Damper*. MS thesis. Virginia Polytechnic Institute and State University.

18. Vamvatsikos, D. (2006) Incremental dynamic analysis with two components of motion for a 3D steel structure. *Proceedings of the 8th U.S. National Conference on Earthquake Engineering*, San Francisco.

19. Asgarian, B., Sadrinezhad, A., and Alanjari, P. (2010) Seismic performance evaluation of steel moment-resisting frames through incremental dynamic analysis. *Journal of Constructional Steel Research*, **66**, 178-190.

20. Cheraghi Afarani, M.H. and Nicknam, A. (2012) Assessment of collapse safety of stiffness irregular SMRF structures according to IDA approach. *Journal of Basic and Applied Scientific Research*, **2**(7), 6563-6573.

21. Pacific Earthquake Engineering Research Center (PEER) (2000) *PEER Strong Motion Database*. University of California, Berkeley. Available: http://peer.berkeley.edu/smcat/search.html [2012, November10]

22. National Iranian Code of Minimum Building Loads, Standard No.519-2000.

23. Building and Housing Research Center (2004) *Iranian Code of Practice for Seismic Resistant Design of Buildings*. Standard No. 2800, 3rd Edition.

24. *Manual of SeismoStruct-V5* [online]. Available: http://www.SeismoSoft.com/ [2012, December 23].

25. Mari, A. and Scordelis A. (1984) *Nonlinear Geometric Material and Time Dependent Analysis of Three Dimensional Reinforced and Prestressed Concrete Frames*. Report SESM 82–12, Department of Civil Engineering, University of California, Berkeley.

26. Neuenhofer, A. and Filippou, F.C. (1997) Evaluation of nonlinear frame finite-element models. *Journal of Structural Engineering*, **123**(7), 958-966.

Nomenclature

IDA: Incremental dynamic analysis
IM: Intensity Measure
DM: Damage Measure
PGA: Peak Ground Acceleration
PGV: Peak Ground Velocity
M_w: Moment magnitude
T_p: Pulse period
r: fault distance
ς_p: damping ratio
ω_p: pulse frequency
s: the maximum amplitude of velocity time history
R: real records
DS: decaying sinusoidal records
IO: Immediate Occupancy
CP: Collapse Prevention
SMRF: Steel Moment Resisting Frame